

# UCSF

## UC San Francisco Previously Published Works

### Title

Shear strain and inflammation-induced fixed charge density loss in the knee joint cartilage following ACL injury and reconstruction: A computational study

### Permalink

<https://escholarship.org/uc/item/8sp846q2>

### Journal

Journal of Orthopaedic Research®, 40(7)

### ISSN

0736-0266

### Authors

Orozco, Gustavo A  
Eskelinen, Atte SA  
Kosonen, Joonas P  
[et al.](#)

### Publication Date

2022-07-01

### DOI

10.1002/jor.25177

Peer reviewed



Published in final edited form as:

*J Orthop Res.* 2022 July ; 40(7): 1505–1522. doi:10.1002/jor.25177.

## Shear strain and inflammation-induced fixed charge density loss in the knee joint cartilage following ACL injury and reconstruction: a computational study

Gustavo A. Orozco<sup>\*,a,b</sup>,

Atte S.A. Eskelinen<sup>\*,a</sup>,

Joonas P. Kosonen<sup>a</sup>,

Matthew S. Tanaka<sup>c</sup>,

Mingrui Yang<sup>d</sup>,

Thomas M. Link<sup>c</sup>,

Benjamin Ma<sup>c</sup>,

Xiaojuan Li<sup>d</sup>,

Alan J. Grodzinsky<sup>e</sup>,

Rami K. Korhonen<sup>a</sup>,

Petri Tanska<sup>a</sup>

<sup>a</sup>Department of Applied Physics, University of Eastern Finland, Kuopio, Finland Yliopistonranta 1, FI-70210 Kuopio, Finland

<sup>b</sup>Department of Biomedical Engineering, Lund University, Box 188, 221 00, Lund, Sweden

<sup>c</sup>Department of Radiology and Biomedical Imaging, University of California, San Francisco, 1500 Owens St, San Francisco, CA 94158, USA

<sup>d</sup>Department of Biomedical Engineering, Lerner Research Institute, Program of Advanced Musculoskeletal Imaging (PAMI), 9500 Euclid Avenue, Cleveland Clinic, Cleveland, OH 44195, USA

<sup>e</sup>Departments of Biological Engineering, Electrical Engineering and Computer Science and Mechanical Engineering, Massachusetts Institute of Technology, Cambridge, MA, USA

### Abstract

**Corresponding author:** Gustavo A. Orozco, *Department of Applied Physics, University of Eastern Finland, Kuopio, Finland, Yliopistonranta 1, 70210 Kuopio, FI, Tel: +358 50 3485018, gustavo.orozco@uef.fi.*

\*These authors contributed equally

**Author Contributions:** G.O. research design, acquisition, analysis, interpretation, manuscript drafting, and revision. A.E. research design, acquisition, analysis, interpretation, manuscript drafting, and revision. J.K. acquisition, analysis, manuscript drafting, and revision. M.T. acquisition, analysis, manuscript revision. M.Y. acquisition, analysis, manuscript revision. T.L. acquisition, analysis, manuscript revision. B.M. acquisition, analysis, interpretation, manuscript revision. X.L. research design, analysis, interpretation, manuscript revision. A.G. research design, analysis, interpretation, manuscript drafting, and revision. R.K. research design, analysis, interpretation, manuscript drafting, and revision. P.T. research design, analysis, interpretation, manuscript drafting, and revision. All authors have read and approved the final submitted manuscript.

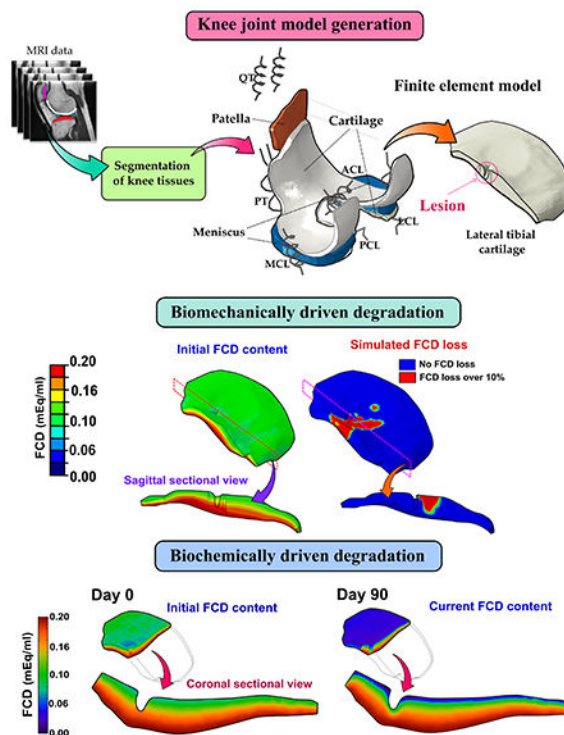
Conflict of interest

The authors declare no potential conflict of interest.

Excessive tissue deformation near cartilage lesions and acute inflammation within the knee joint after anterior cruciate ligament (ACL) rupture and reconstruction surgery accelerate the loss of fixed charge density (FCD) and subsequent cartilage tissue degeneration. Here, we show how biomechanical and biochemical degradation pathways can predict FCD loss using a patient-specific finite element model of an ACL reconstructed knee joint exhibiting a chondral lesion. Biomechanical degradation was based on the excessive maximum shear strains that may result in cell apoptosis, while biochemical degradation was driven by the diffusion of pro-inflammatory cytokines. We found that the biomechanical model was able to predict substantial localized FCD loss near the lesion and on the medial areas of the lateral tibial cartilage. In turn, the biochemical model predicted FCD loss all around the lesion and at intact areas; the highest FCD loss was at the cartilage–synovial fluid-interface and decreased towards the deeper zones. Interestingly, simulating a downturn of an acute inflammatory response by reducing the cytokine concentration exponentially over time in synovial fluid led to a recovery of FCD content in the cartilage. Our novel numerical approach suggests that *in vivo* FCD loss can be estimated in injured cartilage following ACL injury and reconstruction. *Significance:* Our novel modeling platform can benefit the prediction of PTOA progression and the development of treatment interventions such as disease-modifying drug testing and rehabilitation strategies.

### Graphical Abstract

Biomechanical and biochemical degradation models were utilized to estimate FCD loss using a patient-specific finite element model of an ACL reconstructed knee joint. Biomechanical degradation was based on the excessive maximum shear strains that may result in cell apoptosis, while biochemical degradation was driven by the diffusion of pro-inflammatory cytokines. The biomechanical model predicted substantial localized FCD loss near the lesion and on the medial areas of the lateral tibial cartilage. In turn, the biochemical model predicted FCD loss all around the lesion and also at intact areas.



## Keywords

post-traumatic osteoarthritis; inflammation; diffusion; finite element model; ACL reconstruction; fixed charge density; Biomechanics; Cartilage; Finite Element Analysis; Inflammation; Mechanobiology; Osteoarthritis - Post Traumatic; Cytokines

## Introduction

Anterior cruciate ligament (ACL) rupture is one of the most common traumatic knee joint injuries which often promotes the predisposition of other tissues such as menisci and articular cartilage to damage and development of post-traumatic osteoarthritis (PTOA). Signs of this disease include the appearance of fibrocartilaginous tissue, loss of fixed charge density (FCD) associated with proteoglycans (PGs) especially near acute osteochondral lesions, and an increase of inflammatory biomarkers in the synovial fluid. Every year in the United States, about 200,000 ACL injuries are reported of whom more than 70% are estimated to receive surgical ligament reconstruction<sup>1–3</sup> which aims to restore the normal biomechanical function of the joint and prevent further tissue deterioration. However, even successful ACL reconstruction (ACLR) does not always prevent the onset of PTOA.<sup>4</sup>

Although ACLR surgery is considered to restore the biomechanical environment of the knee<sup>5</sup>, cartilage is often injured and formation or worsening of chondral lesions is inevitable despite surgery. The location and morphology of chondral lesions also modulate the mechanical response of cartilage.<sup>6</sup> These responses include, for example, higher susceptibility to shear deformation near lesions during normal gait<sup>7,8</sup> which may

lead to chondrocyte death and accelerated FCD loss<sup>9-11</sup>. Furthermore, despite or due to ACLR surgery<sup>12</sup>, the acute changes in the knee joint trigger an inflammatory response in the joint. This inflammatory response is driven by the introduction and diffusion of cytokines (such as pro-inflammatory interleukins IL-1 or IL-6) which increase the levels of proteolytic enzymes such as the aggrecanases (ADAMTS-4,5 a disintegrin and metalloproteinase with thrombospondin motifs) in the synovial fluid and cartilage that degrade aggrecan PGs. Cytokines can also reduce the synthesis of extracellular matrix components (aggrecan, collagen)<sup>13</sup>. Eventually, these changes accelerate cartilage degradation, ultimately decreasing the intra-tissue FCD levels.<sup>14-18</sup> The interaction between biomechanical and biochemical degradation mechanisms might disturb the healthy balance between anabolic and catabolic states of the tissue, possibly leading to irreversible worsening of cartilage condition<sup>19</sup>.

Comprehension of these degradation mechanisms, and how they change over time, is important for the development of more successful strategies for the prevention of PTOA progression after ACLR. Previous numerical knee joint<sup>20-22</sup> and *in vitro* models<sup>9,11,23,24</sup> have shed some light on cartilage degradation after injury. Particularly, in our previous joint-level work<sup>7</sup>, a biomechanical degeneration algorithm could predict FCD loss near a lesion corresponding to MRI findings, but the model could not explain alterations of cartilage composition away from lesions as suggested by quantitative MRI. Also, clinical studies have reported fluctuations in the synovial fluid cytokine concentrations over time<sup>25,26</sup>. Together these observations underline the need for refining joint-level models to also incorporate biochemical degradation mechanisms. Establishing a robust procedure to estimate both biomechanical and inflammation-related alterations in cartilage over time could lead to the development of tools for patient-specific planning of effective rehabilitation schemes.

In this study, we implemented a biochemical FCD degeneration mechanism into a patient-specific finite element model of the ACL reconstructed knee joint to estimate FCD loss in injured cartilage. The biochemical degeneration was based on the diffusion of pro-inflammatory cytokines into tissue and the net effect of the subsequent release of degradative ADAMTS-4,5 and protective TIMP-3 (tissue inhibitor of metalloproteinase-3)<sup>16,18</sup>. Then, we compared our results with the predictions of a previous biomechanical FCD degeneration model in which the degeneration was based on the excessive maximum shear strain.<sup>7</sup> To overcome the lack of information about *in vivo* biochemical response of human cartilage to an inflamed environment, we also conducted a sensitivity analysis by varying pro-inflammatory cytokine concentration, aggrecanase catalytic rate, and aggrecan biosynthesis rate. We consider these parameters as the most influential on the biochemical FCD loss based on our preliminary tests. We hypothesized that **i**) biochemical interactions cause FCD loss over larger areas due to synovial fluid distributing inflammatory cytokines to all cartilage surfaces, and that **ii**) reduction in the synovial fluid cytokine levels with time after the acute phase (simulating diminished inflammation in time) will start a recovery process of FCD content in the cartilage.

## Methods

### Knee joint model generation and biomechanical cartilage degradation.

In our previous study<sup>7</sup>, we investigated the development of a patient-specific knee joint model and the implementation of a biomechanical degradation algorithm, which we briefly describe here to help compare these biomechanical and biochemical degradation models. For additional information, the reader is referred to Supplementary material Section A. First, a patient with an ACL reconstructed knee (44 years, 79 kg) was imaged at a 1-year follow-up time point using a clinical MRI scanner (3.0T, MR750w, General Electric Healthcare). This time point was used to obtain joint tissue geometries and implement the initial cartilage composition in the biochemical finite element (FE) model. Simultaneous acquisition of  $T_{1\rho}/T_2$  relaxation times was performed to quantify the  $T_{1\rho}$  and  $T_2$  cartilage maps at the knee joint cartilage 1 and 3 years after surgery. Second, gait analysis and musculoskeletal modeling of the subject were used to provide knee joint input to the FE joint model constructed in ABAQUS (v2018, Dassault Systèmes Simulia Corp., Providence, USA).

For the biomechanical degradation model, a previously developed degeneration algorithm<sup>9,11</sup> driven by maximum shear strain (damage threshold: 40%) was utilized to predict FCD loss in cartilage during the stance phase of the gait via consecutive loading iterations (see Supplementary material Section B for additional information about the biomechanical degradation approach).

### Biochemically-induced cartilage degradation model.

For simulations of biochemical degradation, we assumed the global changes in the biochemical properties were similar for both femoral and tibial cartilages. Thus, only the lateral tibial cartilage (including chondral lesion) was considered for studying the chondral lesion environment. Furthermore, we assumed that the majority of FCD content originates from aggrecan in the extracellular matrix; hence we used diffusion parameters for aggrecan (and not other smaller PGs) to model changes in FCD. The cartilage geometry was meshed using 4-node tetrahedral elements in ABAQUS and imported into COMSOL Multiphysics (version 5.3a, Burlington, MA, USA). A previous time-dependent reaction-diffusion model<sup>16,18</sup> was employed to simulate FCD loss via diffusion of pro-inflammatory cytokines through the free surfaces (all surfaces excluding the cartilage–bone-interface) of tibial cartilage. Since biochemical properties for human cartilage are not well-known and those might have subject-specific variation, model parameters (such as diffusion and catalytic rate coefficients of ADAMTS-4,5) were obtained from a previous *in vitro* study, in which a similar model was calibrated to IL-1-induced degeneration in young bovine explants.<sup>27</sup> In addition, the reported human depth-dependent aggrecan distribution<sup>28,29</sup> was implemented into the model.

As biochemical boundary conditions, a constant pro-inflammatory cytokine concentration of 94 pg/ml (adopted from the IL-6 concentration in the patient's synovial fluid on the day of ACLR surgery<sup>17</sup>) was set on the free surfaces (top, lesion, and lateral; Dirichlet boundary condition). Also, the aggrecanase concentration was set to 0 pg/ml on the free and bottom surfaces, and the mass transfer of intact aggrecan was allowed through the

free surfaces in order to consider the diffusion of aggrecan out of the cartilage to the synovial fluid<sup>19</sup>. In contrast, diffusion was restricted for any of the chemical species through the cartilage-bone interface. The chondrocyte concentration<sup>30</sup> was constant throughout the simulation (spatially and temporally), and neither apoptosis nor necrosis was included due to a lack of experimental data about the rate of chondrocyte death. The total diffusion time was set to 90 days to obtain a relatively early-phase response when analyzing the effect of the model parameters on the FCD concentrations. Over this timescale, the knee joint cytokine concentrations of ACLR patients are still above healthy control levels of unoperated knees<sup>31</sup>. Moreover, clinical studies report similar collection times of synovial fluid samples from ACLR patients<sup>31,32</sup>.

### Pro-inflammatory cytokine diffusion model.

The diffusion of pro-inflammatory IL-1/IL-6/TNF $\alpha$  into poroelastic tissue and proteolytic effects of aggrecanases were modeled with parabolic reaction-diffusion partial differential equations<sup>16,33</sup>

$$\frac{\partial C_j}{\partial t} = D_j \nabla^2 C_j \pm R_j, \quad (1)$$

where  $C_j$  is the concentration/amount of the constituent  $j$ ,  $t$  is time,  $D_j$  is the effective diffusivity of the chemical species  $j$  and  $R_j$  is the corresponding source/sink term, which describes the rate of generation/repair or degradation of the species. The species  $j$  include chondrocytes (spatially and temporally constant), pro-inflammatory cytokines, intact aggrecans, and aggrecanases. The model reflects the net effect of pro-inflammatory cytokines IL-1, IL-6, and TNF $\alpha$ , and we assumed the diffusion and catabolic properties of IL-6 and TNF $\alpha$  to be similar to experimentally validated IL-1 properties.<sup>16</sup> The catabolic activity of aggrecanases was also implemented as a net effect of ADAMTS-4,5 and TIMP-3.<sup>16</sup> The source/sink terms  $R_j$  to describe the proteolytic effect of aggrecanases on aggrecan content were designed in accordance with Michaelis—Menten kinetics. For the case of intact aggrecan, the Eq. (1) takes the following form:

$$\frac{\partial C_{\text{agg}}}{\partial t} = D_{\text{agg}} \nabla^2 C_{\text{agg}} - \gamma_1 R_{\text{aggrecan cleaved by aggrecanases}} + \gamma_2 R_{\text{aggrecan synthesis}}, \quad (2)$$

where  $C_{\text{agg}}$  is the intact aggrecan concentration,  $D_{\text{agg}}$  is the effective diffusivity of aggrecan,  $\gamma_1$  is aggrecanase catalytic rate coefficient,  $R_{\text{aggrecan cleaved by aggrecanases}}$  is the sink term for the catalytic activity of aggrecanases cleaving aggrecan,  $\gamma_2$  is the aggrecan biosynthesis rate multiplier, and  $R_{\text{aggrecan synthesis}}$  is the source term for aggrecan biosynthesis (see the Supplementary material Section C and Kar et al.<sup>16,18</sup> for more details).

Experimentally observed time delay in the secretion of ADAMTS after the initiation of biochemical challenge<sup>34</sup> was included in the form of a stimulus expression:

$$\frac{\partial S_{\text{aga}}}{\partial t} = \alpha_{\text{aga}}(C_{\text{r-complex}} - S_{\text{aga}}), \quad (3)$$

where  $S_{aga}$  is a term describing pro-inflammatory cytokine-mediated stimulus response to form aggrecanases (more specifically, the net effect of aggrecanases ADAMTS-4,5 and counteracting TIMP-3),  $C_{r-complex}$  is the concentration of receptor complexes and  $\alpha_{aga}$  is a rate constant for stimulus. This stimulus variable  $S_{aga}$  was used to define source terms  $R_j$  in Eq. (1) for aggrecanases.

In the biochemical model developed in COMSOL Multiphysics, the main degrading constituent is depth-wise intact aggrecan content, having a concentration  $C_{agg}$ . However, to have consistent comparisons of the FCD loss between the biomechanically- and biochemically-driven models, the FCD concentration (mEq/ml) in the biomechanical model was converted to the input parameter of the biochemical model (aggrecan concentration (moles/m<sup>3</sup>)). The FCD content was converted to aggrecan by assuming two moles of negative charge per mole of disaccharide<sup>35</sup> and using the reported molecular weight of 502.5 mg/mmol (assuming the total molecular weight of aggrecan to be 2.5 MDa<sup>36</sup>). These values are representative of the chondroitin sulfate disaccharide, which is the dominant disaccharide in aggrecan.<sup>37</sup> Thus, in terms of FCD, the aggrecan concentration of the cartilage tissue can be calculated with the following equation:

$$C_{agg} = \frac{FCD \cdot 502.5}{-2 \cdot 2.5}, \quad (4)$$

where  $C_{agg}$  is the concentration of intact aggrecan expressed in moles/m<sup>3</sup> and FCD is the fixed charge density of the cartilage tissue expressed in mEq/ml. The FCD concentration was consistent with previously reported values for human adult cartilage tissue.<sup>28,38,39</sup> The COMSOL Multiphysics model results for aggrecan concentration (maximum value: 0.02 moles/m<sup>3</sup>) were then transformed back to the FCD concentration (mEq/ml) using the inverse form of Eq. (4).

### Sensitivity analysis of biochemical model parameters.

We performed an additional analysis in order to determine the sensitivity of biochemical degradation results to the variations in the reaction-diffusion model parameters. First, we considered various pro-inflammatory cytokine concentrations in order to obtain results of the range measured from the patient's synovial fluid on the day of ACLR surgery (IL-1, IL-6, and TNF $\alpha$ ). Second, we studied two additional aggrecanase catalytic rates  $\gamma_1$  (see Eq. (2); extensive details in Kar et al.<sup>16</sup>, where this parameter is denoted as  $k_3$ ) to estimate the effect of aggrecanase aggressiveness on the FCD loss estimations in the model. Third, we analyzed two additional aggrecan biosynthesis rate multipliers  $\gamma_2$  (see Eq. (2)) due to data unavailability for human cartilage tissue. Finally, we simulated an exponential decay of the relative pro-inflammatory cytokine concentration over time starting at day 15 to assess the response of our biochemical model to diminishing inflammatory stress indicating the end of an acute inflammatory response<sup>25,31</sup>. We performed 9 biochemical simulations under variations of reaction-diffusion parameters within the ranges shown in Table 1. According to our preliminary analyses, the cartilage response to cytokines was similar in the healthy areas near the lesion and further away from the lesion. Therefore, spatial and temporal FCD concentrations were evaluated only across and at the edge of the cartilage lesion (~ 3 mm).



The computational workflow developed in this study is shown in Figure 1.

## Results

### Biomechanical cartilage degradation.

Our previous biomechanical degeneration model<sup>7</sup> showed areas in the tibial plateau cartilage where the maximum shear strain exceeded the thresholds of FCD loss. The highest maximum shear strain was obtained at the second peak of the stance phase (~0.75 stance fraction). In that previous investigation, the shear strain-driven model predicted localized FCD loss near the lesion and on the central surface of the lateral tibial cartilage (Figure 2A). After 50 iterations, this model estimated an average relative decrease of 7.8 % in the FCD content with respect to the initial FCD distribution in the whole lateral tibial cartilage domain (Table 2).

### Biochemical cartilage degradation.

Our biochemical model predicted a substantial and similarly distributed FCD loss in the intact cartilage regions. The FCD loss was the greatest at the cartilage–synovial fluid-interface and it progressed to the intermediate zone of cartilage after 90 days of simulation time (Figure 3C). Specifically, the superficial zone of cartilage and areas around the lesion experienced degradative biochemical perturbations of the non-fibrillar matrix homeostasis (Figure 2B). In the reference model, the average relative FCD loss in the whole lateral tibial cartilage geometry was 29.5 % compared to the initial FCD distribution (Table 2).

Sensitivity analysis of the model parameters revealed that by increasing the pro-inflammatory cytokine concentration, the FCD content near the cartilage surface was considerably decreased compared to the reference model (Figure 3). As time progressed, the FCD content also reached a steady-state for low cytokine concentrations, while the FCD content distributions were varied faster and decreased more throughout the tissue thickness for high cytokine concentrations (Figure 4). Furthermore, the increase of the aggrecanase catalytic rate  $\gamma_1$  showed a substantial decrease in the FCD content when compared to the reference model (Figure 5). When the aggrecanase catalytic activity was turned off, the FCD content decreased only slightly over time (caused by passive diffusion of PGs out of tissue; this choice also led to steady-state in the simulations). In turn, a large catalytic rate ( $9 \text{ s}^{-1}$ ) caused a substantial decrease in the FCD content throughout the tissue thickness (Figure 6).

Decreasing the aggrecan biosynthesis rate multiplier  $\gamma_2$  increased the FCD loss when compared to the reference model (Figure 7). Conversely, the temporal FCD distributions revealed that for a greater rate multiplier of 2, the cartilage FCD loss was diminished when compared to the reference conditions (and the steady-state was reached faster; Figure 8).

The time-dependent exponential decay of the pro-inflammatory cytokine concentration in the synovial fluid exhibited a similar response to the reference model (constant cytokine concentration) until day 30. Afterward, the FCD content recovered ~7% until day 90 in the model with time-dependent cytokine levels compared to the reference model with constant cytokine concentration over 90 days (Figure 9). The average relative FCD losses

in the whole lateral tibial cartilage after 90 days estimated in all sensitivity analyses are summarized in Table 2.

### Comparison between $T_{1\rho}$ and $T_2$ maps and numerical predictions.

The  $T_{1\rho}$  and  $T_2$  relaxation times increased in the lateral tibial cartilage after ACLR surgery from 1- to 3-year follow-up time points. These alterations were located near the lesion and in the superficial layer of the cartilage tissue. The numerical predictions from biomechanical and biochemical mechanisms corresponded with MRI maps; both showed that the FCD loss was near the lesion. Additionally, the biochemical model predicted FCD loss also away from the lesion in the superficial cartilage (Figure 2C).

## Discussion

In the present study, we developed a biochemical numerical model to estimate cartilage degeneration processes via FCD loss in ACL reconstructed knee. To the best of our knowledge, combined with our previous study<sup>7</sup>, this is the first 3D knee joint model that shows prediction of the progression of PTOA and accounts for either biomechanically or biochemically-driven mechanism for FCD loss. For the biomechanical process, cartilage FCD loss has been simulated under the patient's stance phase of gait by utilizing elevated levels of maximum shear strain as a trigger for PTOA progression.<sup>7</sup> For the biochemical process, a reaction-diffusion model was employed to simulate the FCD loss under the effects of pro-inflammatory cytokines and aggrecanases. Furthermore, a parametric analysis determined the sensitivity of biochemical degradation results to the variations in the reaction-diffusion model parameters.

The biomechanically driven degeneration model predicted a substantial localized FCD loss near the lesion and on the medial areas of the lateral tibial cartilage<sup>7</sup>. In turn, besides in the vicinity of the lesion, the biochemically driven degeneration model predicted FCD loss at the superficial zone of the geometrically intact areas. These numerical results indicate that the experimentally observed alterations in cartilage integrity after ACL injury and reconstruction<sup>40,41</sup> could be due to loss of FCD caused by the biomechanical (excessive shearing) and/or biochemical (elevated levels of inflammatory cytokines) degradation mechanisms<sup>17,25</sup>. These mechanisms might be acting simultaneously or to different degrees possibly at different areas on the cartilage, but this was beyond the scope of the current study. The additional parametric analysis revealed that, as expected, increasing pro-inflammatory cytokine concentration increased the FCD loss in cartilage, while a decrease in the cytokine concentration gradually reduced the FCD loss (and the FCD loss was almost nonexistent in very small cytokine concentrations). In our model simulating the net effect of several cytokines and proteases, increasing the aggrecanase catalytic rate demonstrated that even a relatively low concentration of pro-inflammatory cytokines could lead to a severe FCD loss provided that the net amount of synthesized aggrecanases would exhibit highly catabolic behavior. As expected, turning off the aggrecanase activity led to a similar FCD loss as a negligible pro-inflammatory cytokine concentration. Also, decreasing the aggrecan biosynthesis rate multiplier increased the FCD loss in the model.

Our previous study revealed that the biomechanical degenerative model driven by maximum shear strain estimated a decrease in the FCD content near the lesion and on the surface of the cartilage<sup>7</sup>. Those results were in accordance with previous *in vivo* studies<sup>42,43</sup>, numerical models<sup>11,20,22</sup>, and clinical assessments<sup>17,40</sup> in which excessive strains have been suggested to contribute to the cell apoptosis and breakdown of cartilage extracellular matrix leading to accelerated depletion of aggrecans from the tissue. The biochemical degeneration model showed that FCD content decreased mainly in the superficial layer of the articular cartilage after 90 days. Moreover, our biochemical simulations revealed different FCD content profiles across the lesion compared to the profiles obtained at a short distance from the defect. These differences in the FCD content profiles were due to the higher initial FCD content across the lesion, impeding the effective cytokine diffusion into the cartilage (the effective diffusion coefficient of cytokines depended on aggrecan concentration, see Supplementary material Section C). Substantial FCD loss displayed in our biochemical model was in good agreement with previous experimental studies that have described markedly increased aggrecan loss in injured and cytokine-cultured cartilage.<sup>44,45</sup>

The MRI maps showed that the  $T_{1\rho}$  and  $T_2$  relaxation times increased near the lesion and in the superficial layer of the cartilage tissue from 1- to 3-year follow-up time points. Unfortunately, the acute phase of inflammation might not be confirmed by an MRI evaluation due to the lack of data from the early follow-up time points. Also, the cytokine levels of this specific patient were unknown, and they most likely changed during the follow-up. Therefore, our approach with time-dependent cytokine levels is a theoretical modeling suggestion to simulate the effect of the downturn of cytokine levels. Interestingly, our results showed that the time-dependent reduction of the cytokine concentration led to similar FCD loss over the first 30 days compared to the reference model (constant cytokine concentration). Subsequently, we observed a moderate recovery in the FCD content over the next 60 days compared to the reference model (Figure 9). This recovery of FCD content was not extremely rapid (at least with the chosen exponential decay function), and, importantly, did not occur immediately after dropping off the cytokine concentration. The reason for this delay is that, despite the possible decrease in aggrecanase synthesis following the decrease in cytokine concentrations, the existing aggrecanase activity is not immediately lost (Supplementary material Eq. 21; aggrecanase concentrations do not explicitly depend on IL concentration but instead these quantities interact via a stimulus equation Eq. 20). A similar delay between the decrease in IL-6 levels and the appearance of aggrecanase-generated aggrecan fragments has been observed in synovial fluid samples of ACLR patients.<sup>31</sup> Thus, if aggrecan degradation and loss occur during the acute inflammation phase, the cartilage is in danger of continued degradation even though the cytokine levels may start to decrease. These findings suggest that the optimal time window for the application of disease-modifying drugs (e.g., broad scope anti-inflammatory glucocorticoids or specific cytokine blockers, like dexamethasone and IL-1Ra, respectively<sup>46,47</sup>), is temporally close to the moment of ACL injury or the follow-on reconstructive surgery. Our model could be helpful to predict these processes. For example, provided that the effect of cytokines could be controlled, the acute inflammatory response would not be prolonged to a chronic state and our model could estimate the restoration of the FCD content. Unfortunately, subject-specific changes in the inflammatory response over time after different joint injuries

remain unknown and they may have a substantial contribution to the overall degeneration process.

Traumatic injuries during sports activities or incisions made on the joint capsule during invasive surgery often trigger the acute inflammatory response. While inflammation is relevant for initiation of the healing process, the acute inflammatory response releases cytokines from synovium to the cartilage via the synovial fluid. Elevated levels of pro-inflammatory cytokines then pose a risk to prolong the insult towards a chronic state. Specific acute inflammatory cytokine profiles could be examined both right after ACL injury and reconstruction surgery.<sup>25,26,48</sup> Additionally, systemic low-grade chronic inflammation in obese patients or alcoholics might tip the biochemical homeostasis to the path of destruction. Our model could be used to probe the best- and worst-case scenarios of surgeries, traumas, low or high-grade inflammation, and drug deliveries after careful validation.

In this computational study, some limitations exist regarding the development of numerical models and specific assumptions. First, tissue knee geometries were based on a single ACL reconstructed patient and it might not represent all aspects at a population level. However, our approach is reasonable for this proof-of-concept work, computationally suggesting two separate mechanisms to explain cartilage FCD loss *in vivo*.

Second, the exact patient-specific biomechanical and biochemical properties of cartilage were unknown. Compositional properties can vary in different subjects and they may also be affected by the acute inflammation response after injury and surgery. These factors alter the local mechanical response and, consequently, the estimated maximum shear strains and FCD loss. The FCD loss estimations might also change if pro-inflammatory cytokines alter the material properties of other knee tissues such as subchondral bone, ligaments, and menisci. Further interaction of multiple degenerative factors such as age, obesity, and different lesion locations must be included to fully comprehend the post-traumatic inflammatory response of the whole joint as an organ. For the future, instead of finding values for all the parameters in each of the patients, it is important to find the most important model parameters and find reasonable estimates for them for example patient cohort-wise. Possible factors behind a cohort separation could include cytokine concentrations, presence of biomarkers of synovitis, size and location of lesions, and changes in gait parameters.

Third, the effect of convection on pro-inflammatory cytokine transport due to dynamic loading was not considered in our approach. It has been shown that the fluid velocity and dynamic loading after injury play an important role during cartilage degradation.<sup>9,49</sup> The diffusion (coefficient) of cytokines in areas of cartilage–cartilage contact and how it is affected by the contribution of fluid pressurization or convection during dynamic loading, and subsequent effects of this loading to mechanical injuries, biosynthesis increase, cell apoptosis/necrosis, and inhibition of the catabolic response of cartilage are poorly understood but should be included in future developments.

Fourth, chondral lesion geometry was segmented at a particular time point and its growth over time was not considered. In future models, propagation of the lesions and the effect of mechanical loading on crack growth in the cartilage should be accounted for as it might

affect the local mechanical response<sup>50</sup> and diffusion conditions of the tissue. Likewise, our models did not consider alterations in the collagen network structure since we assumed that loss of aggrecan FCD would occur before collagen degradation. A combined model considering changes in both FCD and collagen content after injury, mechanisms considered in previous numerical studies<sup>16,24</sup>, will be a part of our future investigations.

Fifth, contrary to the biochemical model, our previous biomechanical approach<sup>7</sup> does not include a physical timescale (in days, months, years). Instead, an arbitrary time was simulated, and 50 iterations used in our estimations could represent thousands of repetitions of walking. Our model should be calibrated against *in vivo* and/or *in vitro* experiments in a time-dependent manner or a probabilistic failure analysis should be conducted.<sup>51</sup> Additional experiments also would provide information for validation of our biochemical model parameters, e.g., analyzing the synovial fluid, urine or serum samples and comparing numerical predictions with alterations in the longitudinal  $T_{1\rho}$  and  $T_2$  relaxation times of injured knee joints.<sup>52</sup>

Sixth, a net degenerative effect of inflammatory cytokines was considered in our biochemical model. As a simplification, we did not simulate the individual catabolic influence for each cytokine that might act after injury. We assumed that simulating each cytokine individually would probably not change that much of our conclusions. On the other hand, if we consider each inflammatory cytokine in our model, then further experimental validation would be costly and time-consuming, and the model would become perhaps unnecessarily complex. Furthermore, we did not consider the apoptotic effect of pro-inflammatory cytokines on the chondrocytes and the subsequent changes in the aggrecan synthesis and the aggrecanase activity in the matrix. These actions of cytokines will be included in the future developments.

Seventh, biomechanical and biochemical degradation mechanisms were investigated independently, while it is reasonable to assume that they might interact. In the future, we plan to combine these two degeneration mechanisms to occur simultaneously and assess our approach in more patients. In order to calibrate these models, more experimental data combining both biomechanical and biochemical mechanisms are needed to determine model parameters for human tissue, *i.e. in vitro* and *in vivo* diffusion coefficients of cytokines, turnover rate of aggrecan, and biomechanical degeneration rate parameters. All these parameters are most likely age- and/or subject-specific, including material and compositional variations after injury. Nevertheless, we strongly believe that reasonable estimates of FCD loss could be achieved if the most influential parameters could be estimated for example in different patient cohorts.

In conclusion, the results of this numerical modeling study propose that the biomechanically and biochemically driven degeneration mechanisms could explain and be used to estimate the FCD loss in cartilage following ACL injury and reconstruction. Our computational approach is a promising approach which in the future could be utilized as a tool for identifying patients prone to accelerated PTOA progression and planning of rehabilitation and surgical procedures.

## Supplementary Material

Refer to Web version on PubMed Central for supplementary material.

## Acknowledgments

The authors appreciate the support of the University of Eastern Finland, Lund University, the University of California, San Francisco, Cleveland Clinic, and the Massachusetts Institute of Technology to undertake this study. CSC-IT Center for Science Ltd, Finland, is acknowledged for providing software resources. We acknowledge funding support from: The Doctoral Programme in Science, Technology and Computing (SCITECO), the Instrumentarium Science Foundation, the European Union's Horizon 2020 research and innovation programme under the Marie Skłodowska-Curie grant agreement No 713645, Academy of Finland (grant nos. 286526, 324529, 334773 - under the frame of ERA PerMed), Finnish Cultural Foundation (grant #191044), Swedish Research Council (2019-00953 - under the frame of ERA PerMed), Maire Lisko Foundation, Sigrid Juselius Foundation, Päivikki ja Sakari Sohlberg Foundation, Maud Kuistila Memorial Foundation, Saastamoinen Foundation, and from the National Institutes of Health (NIH/NIAMS Grant P50 AR065645 and NIH/NCATS Grant UH3 TR002186) and the American Orthopaedic Society of Sports Medicine (AOSSM) Genzyme Cartilage Initiative grant.

## References

1. Lyman S, Koulouvaris P, Sherman S, et al. 2009. Epidemiology of anterior cruciate ligament reconstruction: trends, readmissions, and subsequent knee surgery. *J Bone Joint Surg Am* 91(10):2321–2328. [PubMed: 19797565]
2. Montalvo AM, Schneider DK, Webster KE, et al. 2019. Anterior Cruciate Ligament Injury Risk in Sport: A Systematic Review and Meta-Analysis of Injury Incidence by Sex and Sport Classification. *J Athl Train* 54(5):472–482. [PubMed: 31009238]
3. Luc B, Gribble PA, Pietrosimone BG. 2014. Osteoarthritis prevalence following anterior cruciate ligament reconstruction: a systematic review and numbers-needed-to-treat analysis. *J Athl Train* 49(6):806–819. [PubMed: 25232663]
4. Allen KD, Golightly YM. 2015. Epidemiology of osteoarthritis: state of the evidence. *Curr Opin Rheumatol* 27(3):276–283. [PubMed: 25775186]
5. Brambilla L, Pulici L, Carimati G, et al. 2015. Prevalence of Associated Lesions in Anterior Cruciate Ligament Reconstruction: Correlation With Surgical Timing and With Patient Age, Sex, and Body Mass Index. *Am J Sports Med* 43(12):2966–2973. [PubMed: 26473010]
6. Jones KJ, Sheppard WL, Arshi A, et al. 2019. Articular Cartilage Lesion Characteristic Reporting Is Highly Variable in Clinical Outcomes Studies of the Knee. *CARTILAGE* 10(3):299–304. [PubMed: 29405742]
7. Orozco GA, Bolcos P, Mohammadi A, et al. 2020. Prediction of local fixed charge density loss in cartilage following ACL injury and reconstruction: a computational proof-of-concept study with MRI. *Journal of Orthopaedic Research* (in press).
8. Bolcos PO, Mononen ME, Tanaka MS, et al. 2019. Identification of locations susceptible to osteoarthritis in patients with anterior cruciate ligament reconstruction: Combining knee joint computational modelling with follow-up T1ρ and T2 imaging. *Clin Biomech (Bristol, Avon)* :104844.
9. Orozco GA, Tanska P, Florea C, et al. 2018. A novel mechanobiological model can predict how physiologically relevant dynamic loading causes proteoglycan loss in mechanically injured articular cartilage. *Scientific Reports* 8(1):15599. [PubMed: 30348953]
10. Trevino RL, Pacione CA, Malfait A-M, et al. 2017. Development of a Cartilage Shear-Damage Model to Investigate the Impact of Surface Injury on Chondrocytes and Extracellular Matrix Wear. *Cartilage* 8(4):444–455. [PubMed: 28934882]
11. Eskelinen ASA, Mononen ME, Venäläinen MS, et al. 2019. Maximum shear strain-based algorithm can predict proteoglycan loss in damaged articular cartilage. *Biomech Model Mechanobiol* 18(3):753–778. [PubMed: 30631999]
12. Li H, Chen C, Chen S. 2015. Posttraumatic knee osteoarthritis following anterior cruciate ligament injury: Potential biochemical mediators of degenerative alteration and specific biochemical markers. *Biomed Rep* 3(2):147–151. [PubMed: 25798238]



13. Dai L, Zhang X, Hu X, et al. 2012. Silencing of microRNA-101 prevents IL-1 $\beta$ -induced extracellular matrix degradation in chondrocytes. *Arthritis Res Ther* 14(6):R268. [PubMed: 23227940]
14. Luli ska-Kuklik E, Maculewicz E, Moska W, et al. 2019. Are IL1B, IL6 and IL6R Gene Variants Associated with Anterior Cruciate Ligament Rupture Susceptibility? *J Sports Sci Med* 18(1):137–145. [PubMed: 30787661]
15. Lieberthal J, Sambamurthy N, Scanzello CR. 2015. Inflammation in joint injury and post-traumatic osteoarthritis. *Osteoarthritis and Cartilage* 23(11):1825–1834. [PubMed: 26521728]
16. Kar S, Smith DW, Gardiner BS, et al. 2016. Modeling IL-1 induced degradation of articular cartilage. *Arch. Biochem. Biophys* 594:37–53. [PubMed: 26874194]
17. Amano K, Huebner JL, Stabler TV, et al. 2018. Synovial Fluid Profile at the Time of Anterior Cruciate Ligament Reconstruction and Its Association With Cartilage Matrix Composition 3 Years After Surgery. *Am J Sports Med* 46(4):890–899. [PubMed: 29364702]
18. Eskelinen ASA, Tanska P, Florea C, et al. 2020. Mechanobiological model for simulation of injured cartilage degradation via pro-inflammatory cytokines and mechanical stimulus. *PLOS Computational Biology* 16(6):e1007998. [PubMed: 32584809]
19. Smith DW, Gardiner BS, Zhang L, Grodzinsky A. 2019. *Articular Cartilage Dynamics*. Springer Singapore, [cited 2019 May 21] Available from: <https://www.springer.com/us/book/9789811314735>.
20. Venäläinen MS, Mononen ME, Salo J, et al. 2016. Quantitative Evaluation of the Mechanical Risks Caused by Focal Cartilage Defects in the Knee. *Scientific Reports* 6:37538. [PubMed: 27897156]
21. Halonen KS, Mononen ME, Töyräs J, et al. 2016. Optimal graft stiffness and pre-strain restore normal joint motion and cartilage responses in ACL reconstructed knee. *Journal of Biomechanics* 49(13):2566–2576. [PubMed: 27370782]
22. Myller KAH, Korhonen RK, Töyräs J, et al. 2019. Computational evaluation of altered biomechanics related to articular cartilage lesions observed in vivo. *J. Orthop. Res* 37(5):1042–1051. [PubMed: 30839123]
23. Mononen ME, Liukkonen MK, Korhonen RK. 2019. Utilizing Atlas-Based Modeling to Predict Knee Joint Cartilage Degeneration: Data from the Osteoarthritis Initiative. *Ann Biomed Eng* 47(3):813–825. [PubMed: 30547410]
24. Mononen ME, Tanska P, Isaksson H, Korhonen RK. 2018. New algorithm for simulation of proteoglycan loss and collagen degeneration in the knee joint: Data from the osteoarthritis initiative. *Journal of Orthopaedic Research* 36(6):1673–1683. [PubMed: 29150953]
25. Struglics A, Larsson S, Kumahashi N, et al. 2015. Changes in Cytokines and Aggrecan ARGS Neopeptide in Synovial Fluid and Serum and in C-Terminal Crosslinking Telopeptide of Type II Collagen and N-Terminal Crosslinking Telopeptide of Type I Collagen in Urine Over Five Years After Anterior Cruciate Ligament Rupture: An Exploratory Analysis in the Knee Anterior Cruciate Ligament, Nonsurgical Versus Surgical Treatment Trial. *Arthritis & Rheumatology* 67(7):1816–1825. [PubMed: 25914389]
26. Bigoni M, Turati M, Gandolla M, et al. 2016. Effects of ACL Reconstructive Surgery on Temporal Variations of Cytokine Levels in Synovial Fluid. *Mediators Inflamm*. 2016:8243601. [PubMed: 27313403]
27. Li Y, Wang Y, Chubinskaya S, et al. 2015. Effects of insulin-like growth factor-1 and dexamethasone on cytokine-challenged cartilage: relevance to post-traumatic osteoarthritis. *Osteoarthritis and Cartilage* 23(2):266–274. [PubMed: 25450855]
28. Han E, Chen SS, Klisch SM, Sah RL. 2011. Contribution of Proteoglycan Osmotic Swelling Pressure to the Compressive Properties of Articular Cartilage. *Biophysical Journal* 101(4):916–924. [PubMed: 21843483]
29. Saarakkala S, Julkunen P. 2010. Specificity of Fourier Transform Infrared (FTIR) Microspectroscopy to Estimate Depth-Wise Proteoglycan Content in Normal and Osteoarthritic Human Articular Cartilage. *Cartilage* 1(4):262–269. [PubMed: 26069557]
30. Jadin KD, Wong BL, Bae WC, et al. 2005. Depth-varying density and organization of chondrocytes in immature and mature bovine articular cartilage assessed by 3D imaging and analysis. *Journal of Histochemistry and Cytochemistry* 53(9):1109–1119. [PubMed: 15879579]

31. Larsson S, Struglics A, Lohmander LS, Frobell R. 2017. Surgical reconstruction of ruptured anterior cruciate ligament prolongs trauma-induced increase of inflammatory cytokines in synovial fluid: an exploratory analysis in the KANON trial. *Osteoarthr. Cartil* 25(9):1443–1451.
32. Larsson S, Lohmander LS, Struglics A. 2009. Synovial fluid level of aggrecan ARGS fragments is a more sensitive marker of joint disease than glycosaminoglycan or aggrecan levels: a cross-sectional study. *Arthritis Res Ther* 11(3):R92. [PubMed: 19545413]
33. Soh S, Byrska M, Kandere-Grzybowska K, Grzybowski B. 2010. Reaction -Diffusion Systems in Intracellular Molecular Transport and Control. *Angew Chem Int Ed Engl* 49(25):4170–4198. [PubMed: 20518023]
34. Chan PS, Caron JP, Orth MW. 2006. Short-term gene expression changes in cartilage explants stimulated with interleukin 1 $\beta$  plus glucosamine and chondroitin sulfate. *Journal of Rheumatology* 33(7):1329–1340. [PubMed: 16821268]
35. Kar S, Smith DW, Gardiner BS, Grodzinsky AJ. 2016. Systems Based Study of the Therapeutic Potential of Small Charged Molecules for the Inhibition of IL-1 Mediated Cartilage Degradation. *PLoS ONE* 11(12):e0168047. [PubMed: 27977731]
36. Nagase H, Kashiwagi M. 2003. Aggrecanases and cartilage matrix degradation. *Arthritis Res. Ther* 5(2):94–103. [PubMed: 12718749]
37. Lesperance LM, Gray ML, Burstein D. 1992. Determination of fixed charge density in cartilage using nuclear magnetic resonance. *Journal of Orthopaedic Research* 10(1):1–13. [PubMed: 1309384]
38. Räsänen LP, Tanska P, Mononen ME, et al. 2016. Spatial variation of fixed charge density in knee joint cartilage from sodium MRI - Implication on knee joint mechanics under static loading. *J Biomech* 49(14):3387—3396. [PubMed: 27667478]
39. Wu Y, Cisewski SE, Sun Y, et al. 2017. Quantifying Baseline Fixed Charge Density in Healthy Human Cartilage Endplate: A Two-point Electrical Conductivity Method. *Spine* 42(17):E1002–E1009. [PubMed: 28699925]
40. Shimizu T, Samaan MA, Tanaka MS, et al. 2019. Abnormal Biomechanics at 6 Months Are Associated With Cartilage Degeneration at 3 Years After Anterior Cruciate Ligament Reconstruction. *Arthroscopy* 35(2):511–520. [PubMed: 30473456]
41. Papatheanasiou I, Michalitsis S, Hantes ME, et al. 2016. Molecular changes indicative of cartilage degeneration and osteoarthritis development in patients with anterior cruciate ligament injury. *BMC Musculoskelet Disord* 17:21. [PubMed: 26762166]
42. Gratz KR, Wong BL, Bae WC, Sah RL. 2008. The effects of focal articular defects on intra-tissue strains in the surrounding and opposing cartilage. *Biorheology* 45(3–43):193–207. [PubMed: 18836224]
43. Guettler JH, Demetropoulos CK, Yang KH, Jurist KA. 2004. Osteochondral defects in the human knee: influence of defect size on cartilage rim stress and load redistribution to surrounding cartilage. *Am J Sports Med* 32(6):1451–1458. [PubMed: 15310570]
44. Li Y, Frank EH, Wang Y, et al. 2013. Moderate dynamic compression inhibits pro-catabolic response of cartilage to mechanical injury, tumor necrosis factor- $\alpha$  and interleukin-6, but accentuates degradation above a strain threshold. *Osteoarthritis and Cartilage* 21(12):1933–1941. [PubMed: 24007885]
45. Stevens AL, Wishnok JS, White FM, et al. 2009. Mechanical injury and cytokines cause loss of cartilage integrity and upregulate proteins associated with catabolism, immunity, inflammation, and repair. *Mol. Cell Proteomics* 8(7):1475–1489. [PubMed: 19196708]
46. Kraus VB, Birmingham J, Stabler TV, et al. 2012. Effects of intraarticular IL1-Ra for acute anterior cruciate ligament knee injury: a randomized controlled pilot trial (NCT00332254). *Osteoarthritis and Cartilage* 20(4):271–278. [PubMed: 22273632]
47. Clements AEB, Murphy WL. 2019. Injectable biomaterials for delivery of interleukin-1 receptor antagonist: Toward improving its therapeutic effect. *Acta Biomaterialia* 93:123–134. [PubMed: 31029831]
48. Bigoni M, Sacerdote P, Turati M, et al. 2013. Acute and late changes in intraarticular cytokine levels following anterior cruciate ligament injury. *J. Orthop. Res* 31(2):315—321. [PubMed: 22886741]



49. Pastrama M-I, Ortiz AC, Zevenbergen L, et al. 2019. Combined enzymatic degradation of proteoglycans and collagen significantly alters intratissue strains in articular cartilage during cyclic compression. *Journal of the Mechanical Behavior of Biomedical Materials* 98:383–394. [PubMed: 31349141]
50. Sadeghi H, Lawless BM, Espino DM, Shepherd DET. 2018. Effect of frequency on crack growth in articular cartilage. *J Mech Behav Biomed Mater* 77:40–46. [PubMed: 28888932]
51. Li W 2016. Damage Models for Soft Tissues: A Survey. *J. Med. Biol. Eng* 36(3):285–307. [PubMed: 27441033]
52. Li X, Cheng J, Lin K, et al. 2011. Quantitative MRI using T1 $\rho$  and T2 in human osteoarthritic cartilage specimens: correlation with biochemical measurements and histology. *Magn Reson Imaging* 29(3):324–334. [PubMed: 21130590]

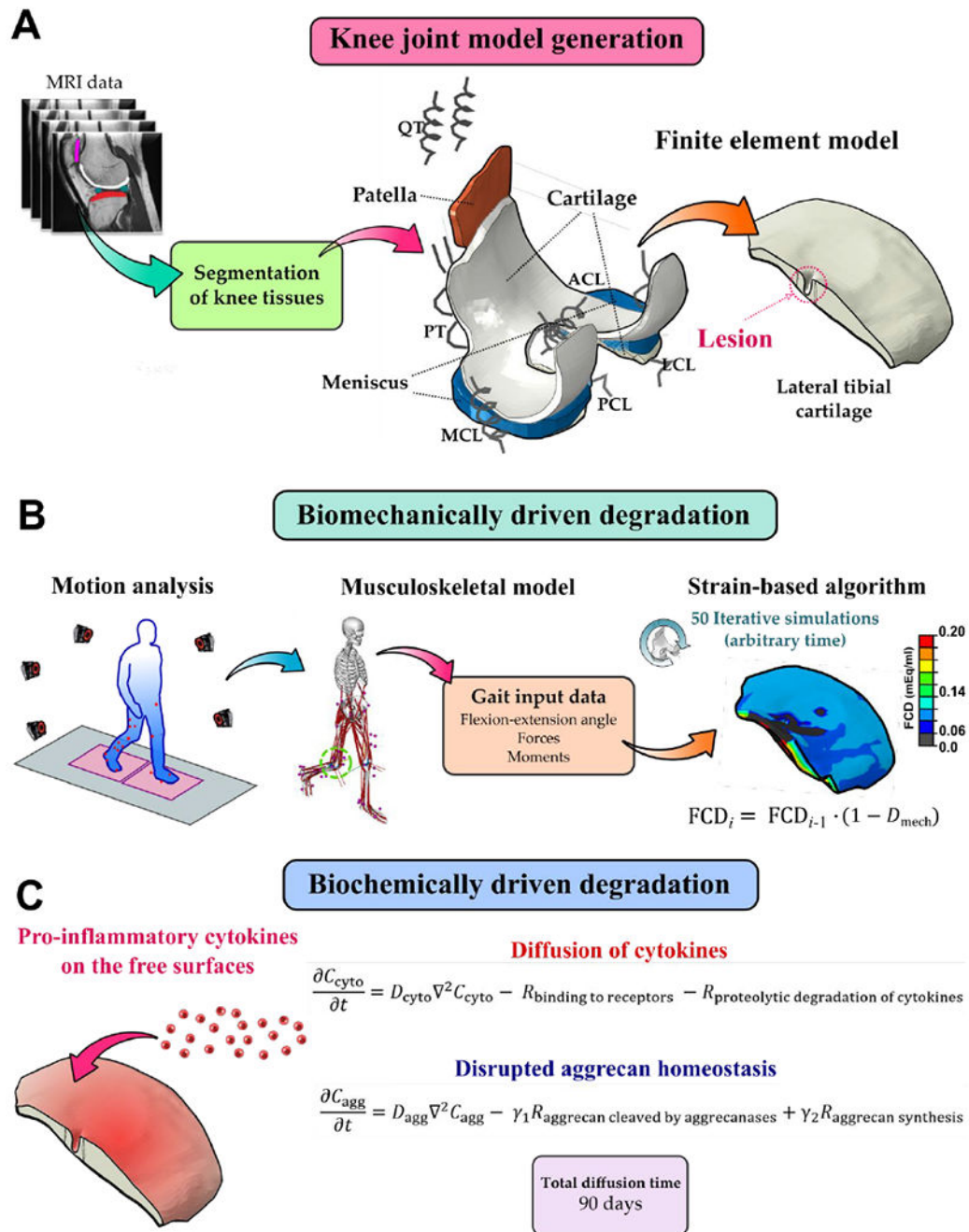


**Figure 1.**

(A) Segmentation of knee tissue geometries for the finite element model, including the cartilage lesion in the lateral tibial cartilage, performed in our previous study<sup>7</sup>. (B) The biomechanical degradation model utilizes patient-specific gait data based on motion analysis, the knee joint biomechanical data obtained from a musculoskeletal model, and an adaptation algorithm driven by excessive maximum shear strain to estimate cartilage FCD loss.<sup>7</sup> (C) The biochemical degradation model considers the diffusion of pro-inflammatory

cytokines into the cartilage as well as the subsequent disruption in aggrecan homeostasis. The total simulation time was 90 days.

Author Manuscript

Author Manuscript

Author Manuscript

Author Manuscript

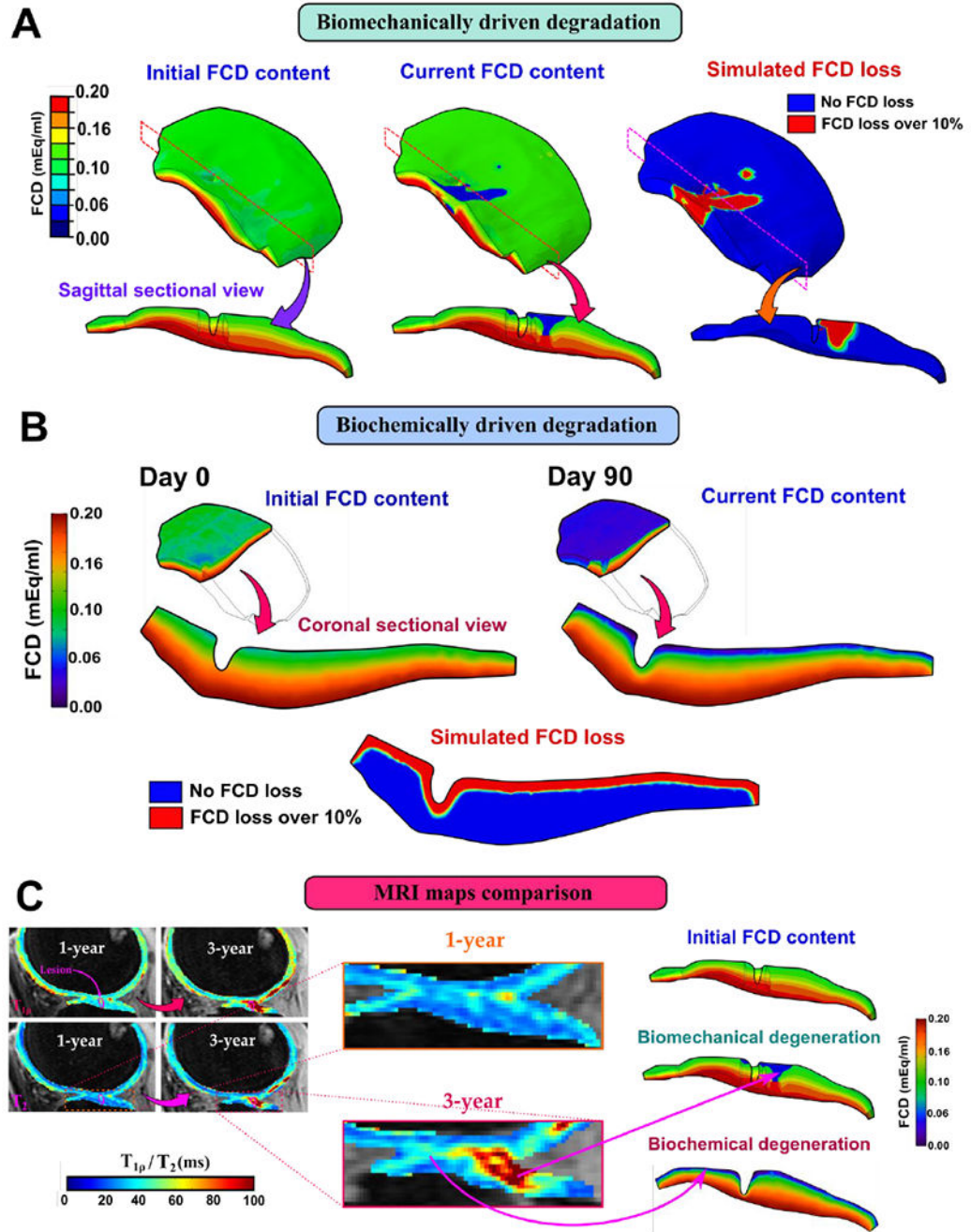


**Figure 2.**

(A) FCD content distributions predicted by the biomechanical model driven by the maximum shear strain mechanism. FCD content reduced on the medial areas of lateral tibial cartilage and around the lesion. (B) The biochemical model predicted substantial FCD loss similarly distributed at the free surfaces of the lateral tibial cartilage, including the tissue lesion. More specifically, the biochemical FCD loss was highest at the cartilage–synovial fluid–interface and decreased towards the inner regions. (C) Sagittal  $T_{1\rho}/T_2$  map slices at both 1- and 3-years follow-up time points for the lateral compartment were used

for qualitative comparison of the numerical biomechanical and biochemical degenerative estimations against *in vivo* findings. Our modeling approach suggests that the biomechanical degradation occurs primarily near the lesion and the intact areas are potentially affected by the biochemical mechanism.

Author Manuscript

Author Manuscript

Author Manuscript

Author Manuscript

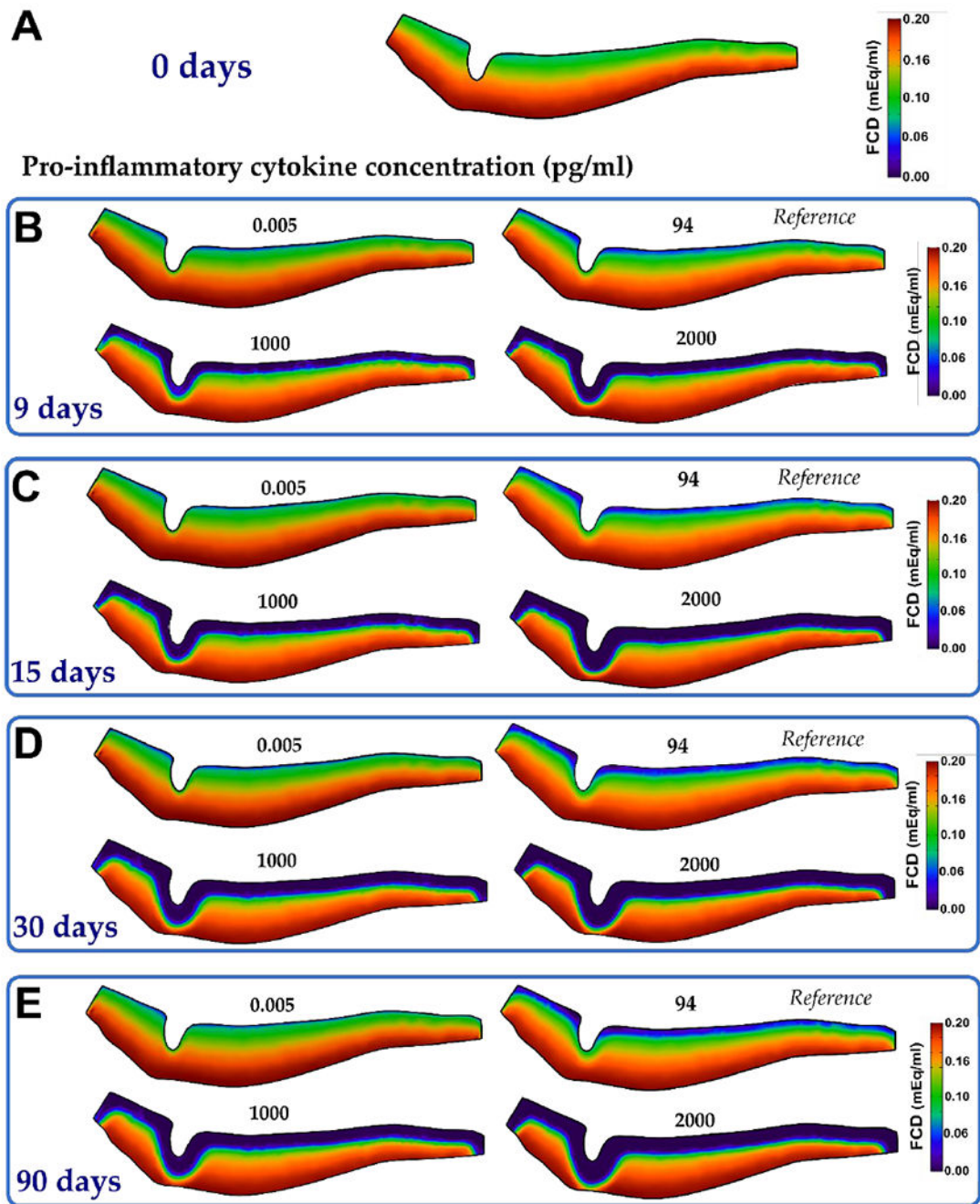


**Figure 3.** Comparison of spatial FCD content distributions across the lateral tibial cartilage subjected to biochemical degradation for different pro-inflammatory cytokine concentrations  $C_{cyto}$  (0.005, 94, 1000 and 2000 pg/ml) at 0, 9, 15, 30 and 90 days.



Pro-inflammatory cytokine concentration (pg/ml)

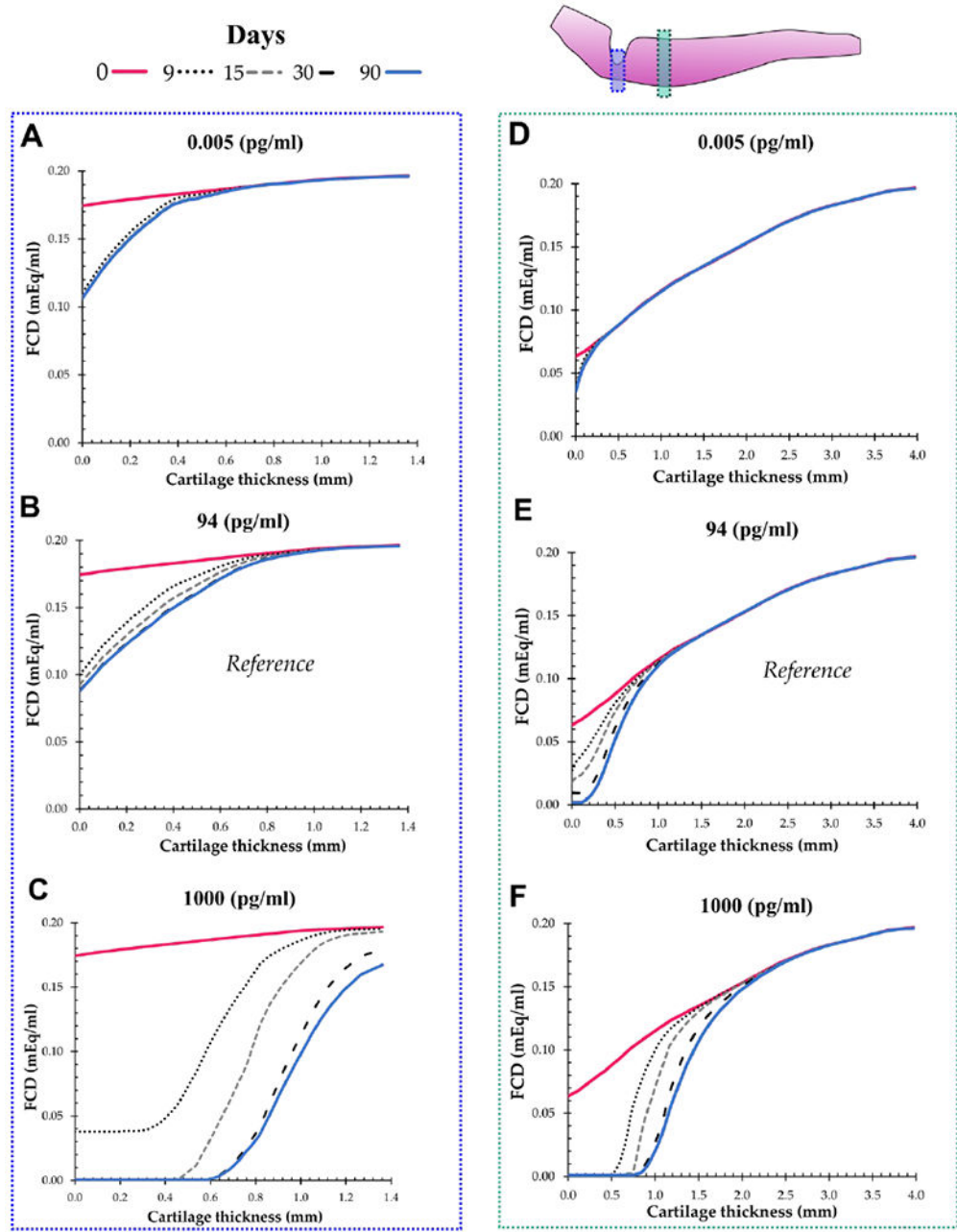


**Figure 4.** Comparison of temporal changes in FCD content across (A-C) and near the edge (D-F) of the lesion within lateral tibial cartilage subjected to biochemical degradation for different pro-inflammatory cytokine concentrations  $C_{cyto}$  (0.005, 94, and 1000 pg/ml) at 0, 9, 15, 30 and 90 days.

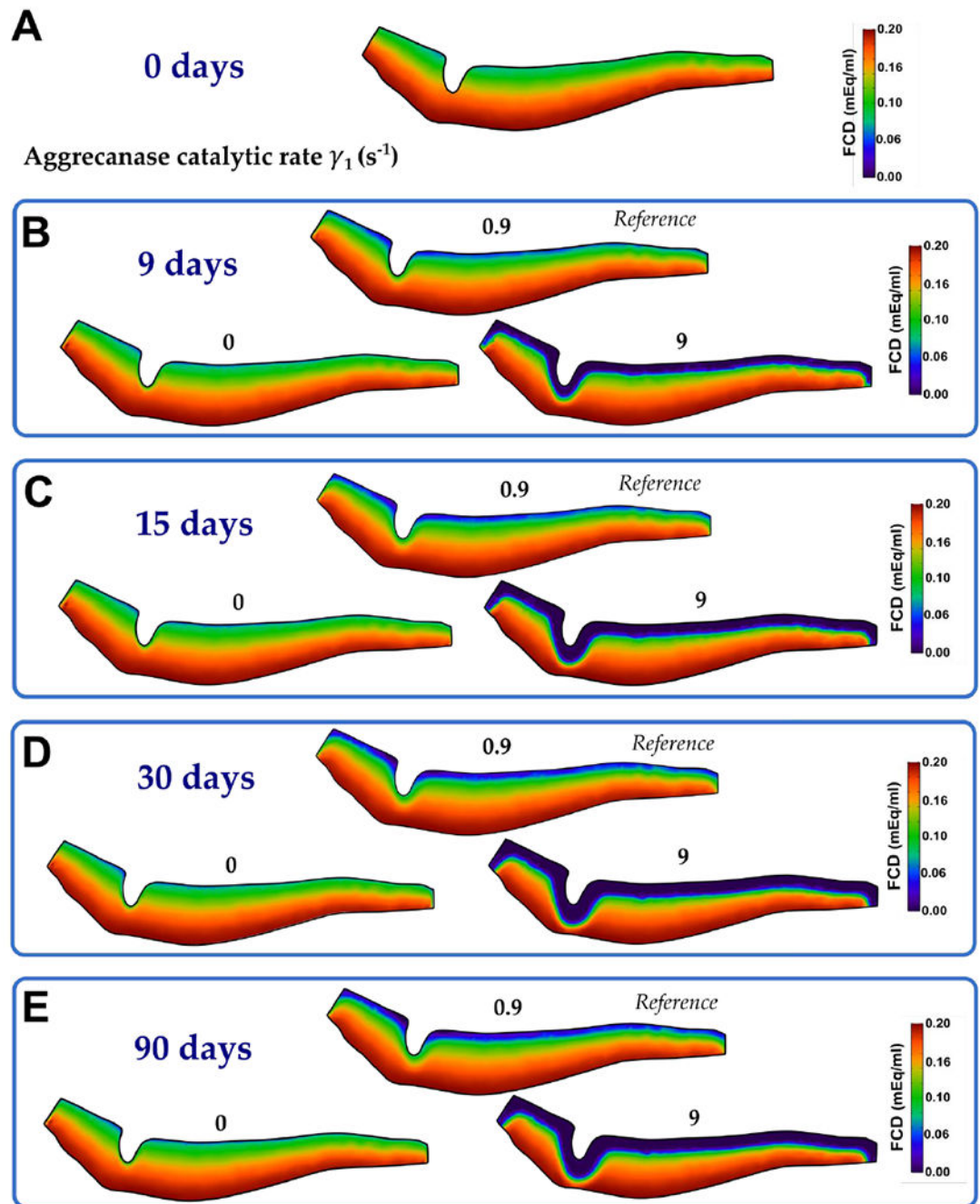


**Figure 5.**

Comparison of spatial FCD content distributions across the lateral tibial cartilage subjected to biochemical degradation for different aggrecanase catalytic rates  $\gamma_1$  (0, 0.9 and 9  $s^{-1}$ ) at 0, 9, 15, 30 and 90 days.



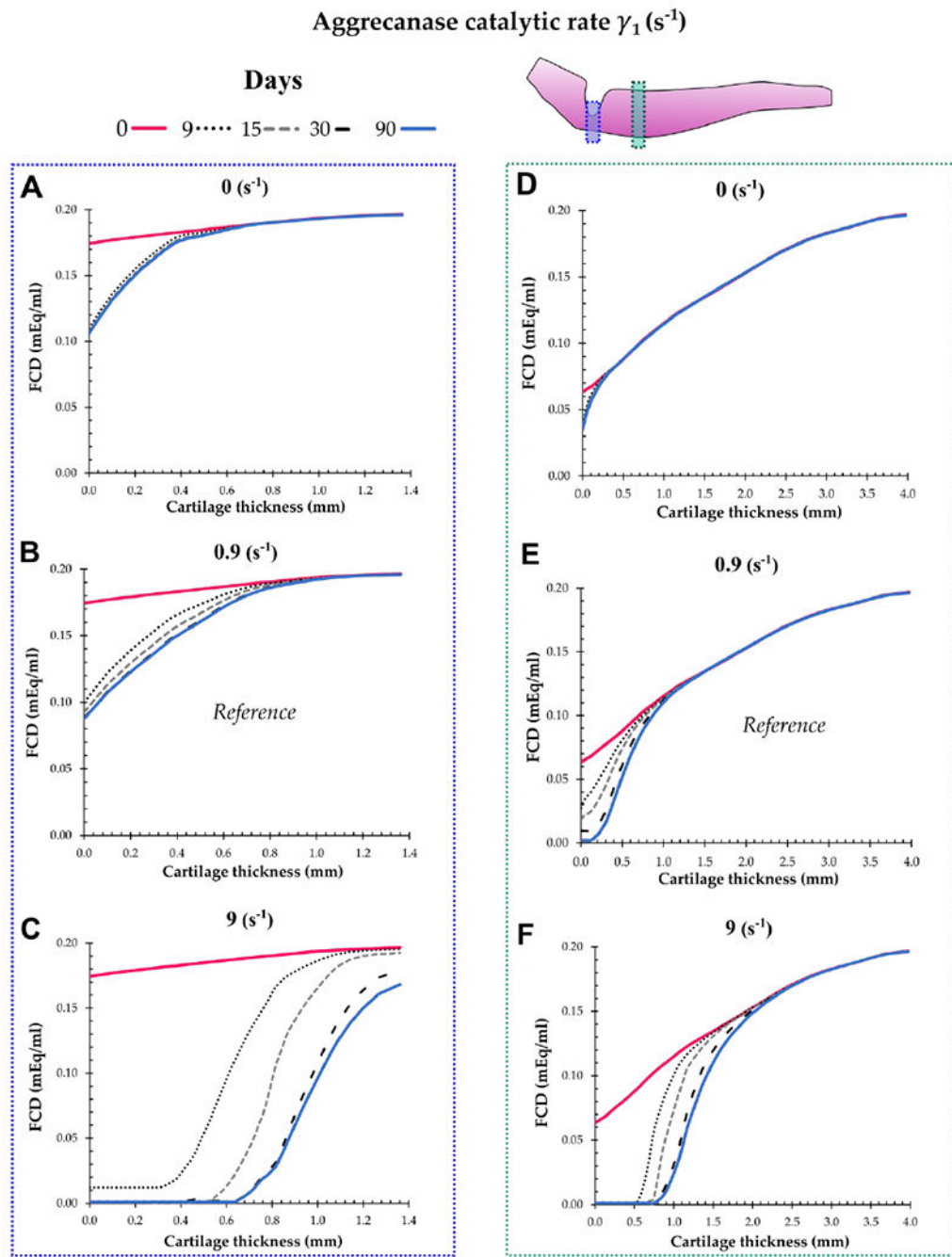


**Figure 6.** Comparison of temporal changes in FCD content across (A-C) and near the edge (D-F) of the lesion within lateral tibial cartilage subjected to biochemical degradation for different aggrecanase catalytic rates  $\gamma_1$  (0, 0.9 and  $9 s^{-1}$ ) at 0, 9, 15, 30 and 90 days.

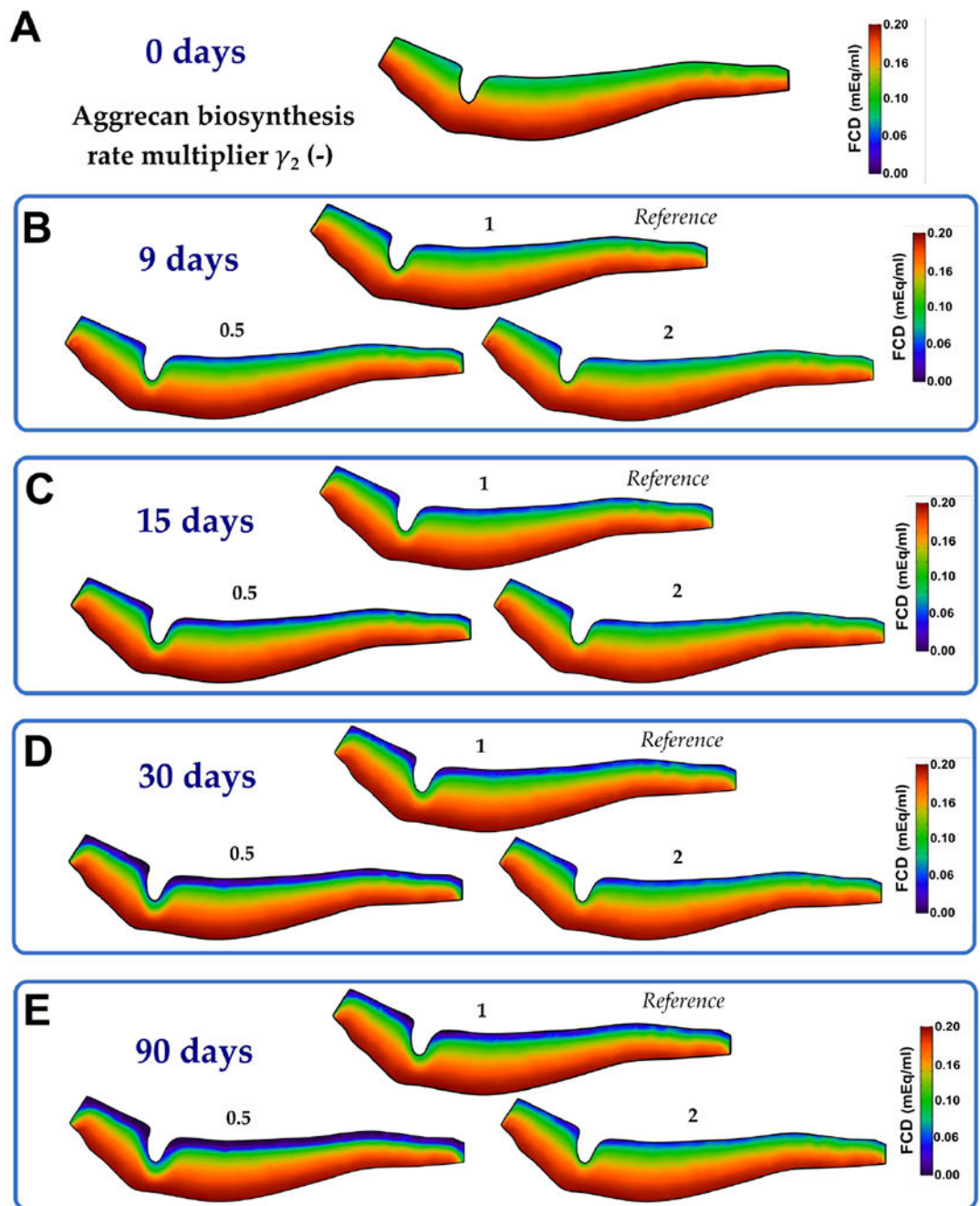


**Figure 7.** Comparison of spatial FCD content distributions across the lateral tibial cartilage subjected to biochemical degradation for different aggrecan biosynthesis rate multipliers  $\gamma_2$  (0.5, 1 and 2) at 0, 9, 15, 30 and 90 days.

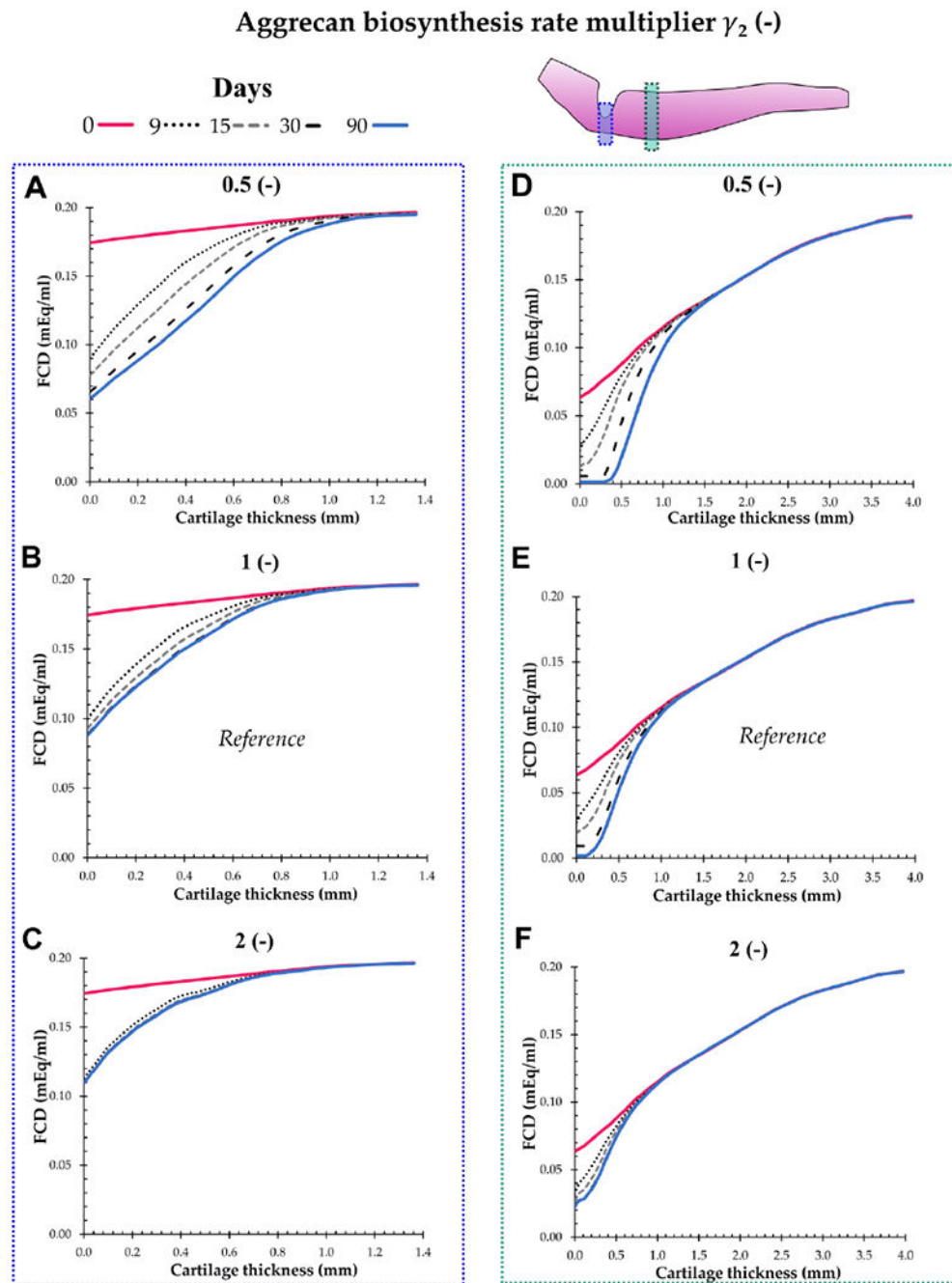


**Figure 8.** Comparison of temporal changes in FCD content across (A-C) and near the edge (D-F) of the lesion within lateral tibial cartilage subjected to biochemical degradation for different aggrecan biosynthesis rate multipliers  $\gamma_2$  (0.5, 1 and 2) at 0, 9, 15, 30 and 90 days.

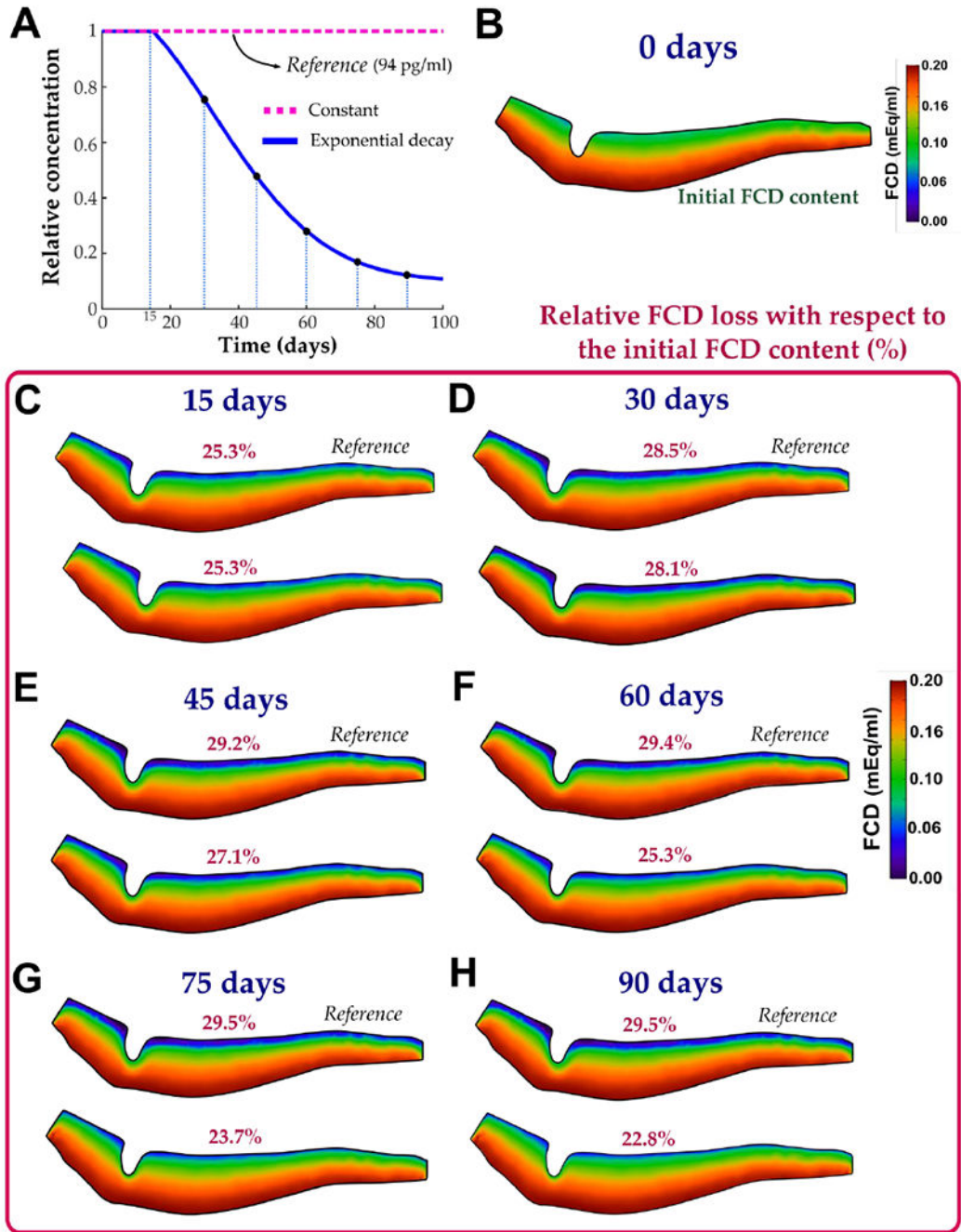


**Figure 9.** (A) An exponential function was implemented to vary the pro-inflammatory cytokine concentration overtime on the free surfaces including the lesion surface. (B-H) Comparison of spatial FCD content distributions across the lateral tibial cartilage subjected to biochemical degradation for the reference setup (temporally constant concentration of 94 pg/ml of pro-inflammatory cytokines) and exponentially decreasing cytokine concentration at 0, 15, 30, 45, 60, 75 and 90 days, respectively. For quantitative comparison, the average

relative percentage of the FCD loss with respect to the initial FCD content over the time has been included.

Author Manuscript

Author Manuscript

Author Manuscript

Author Manuscript

**Table 1**

Summary of the parameters varied in the sensitivity analysis. Bold face elements indicate the reference case for the biochemical degradation model.

Parameter	Range
Pro-inflammatory cytokine concentration $C_{\text{cyto}}$ (pg/ml)	0.005, <b>94</b> , 1000, 2000
Aggrecanase catalytic rate $\gamma_1$ ( $\text{s}^{-1}$ )	0, <b>0.9</b> , 9
Aggrecan biosynthesis rate multiplier $\gamma_2$ (-)	0.5, <b>1</b> , 2
Relative concentration over time (-)	<b>Constant</b> , Exponential decay

**Table 2**

The average relative percentage of the FCD loss estimated from biomechanically and biochemically-driven models with respect to the initial FCD content in the whole lateral tibial cartilage geometry after 50 iterations and 90 days, respectively.

<b>Biomechanically-driven model</b>	<b>7.8</b>
<b>Biochemically-driven model (<i>reference</i>)</b>	<b>29.5</b>
<i>Pro-inflammatory cytokine concentration <math>C_{\text{CytO}}</math> (pg/ml)</i>	
0.005	21.2
1000	51.3
2000	55.6
<i>Aggrecanase catalytic rate <math>\gamma_1</math> (<math>s^{-1}</math>)</i>	
0	21.2
9	52.5
<i>Aggrecan biosynthesis rate multiplier <math>\gamma_2</math> (-)</i>	
0.5	40.2
2	27.1
<i>Relative cytokine concentration over time (-)</i>	
Exponential decay	22.7